Construction of 4D Left Ventricle and Coronary Artery Models

Dong Ping Zhang

Supervisors: Prof Daniel Rueckert, Dr Eddie Edwards

1 Background

Conventional heart surgery is one of the most invasive and traumatic aspects of open-chest surgery, because it requires exposure of the heart and its vessels through median sternotomy. Currently, minimally invasive heart surgery refers to several approaches for bypassing critically blocked arteries. This approach allows access to the heart through small incisions and without stopping the heart, or separating the breastbone and ribcage, or putting the patient on a heart-lung machine during the surgery.

Patients who have minimally invasive procedures instead of conventional open heart surgery have a lower risk of complications associated with the heart-lung machine such as stroke, lung problems, kidney problems, and problems with mental clarity and memory. In addition to reduced complications, by eliminating the need for a painful sternotomy the greatest benefit for the patient is to recover and resume 'normal' activities much quicker than those patients following conventional cardiac surgery.

Figure 1: Chest wall incisions used for a heart surgery (Median sternotomy incision, Minimally invasive approach: partial upper sternotomy, Minimally invasive approach: small right thoracotomy incision) (from Heart & Vascular Institute)

35,986 heart surgeries were performed in UK for the year ending March 2005. These include coronary bypass, repair or replacement of heart valves and many other types of operation, such as repairing holes in the heart, dealing with scars on the heart and diseases of the aorta. 22,166 of them are coronary artery bypass graft (CABG) operations. 3,266 are aortic valve replacement (AVR) operations. Currently, there are three main types of minimally invasive coronary artery bypass procedures: minimally invasive direct coronary bypass (MIDCAB), off-pump coronary artery bypass (OPCAB) and robotic assisted coronary artery bypass (RACAB).

Robotic assisted heart surgery is a type of minimally invasive heart surgery performed by a cardiac surgeon with the support of robotic surgery system (for example, da Vinci robotic surgical system). The surgeon uses a specially-designed computer console to control surgical instruments on thin robotic arms. Robotically-assisted surgery has changed the way certain heart operations are being performed. First, three small incisions or ports are made in the spaces between the ribs. The surgical instruments (attached to the robotic arms) and one camera are placed through these ports. Motion sensors are attached to the robotic wrist, so the surgeon can control the movement of the surgical instruments.

Figure 2: Da Vinci surgical system (adapted from Inc Intuitive Surgical)

Robotically-assisted surgical technique can be used in many heart operations, for example, mitral valve repair and replacement, tricuspid valve repair and replacement, coronary artery bypass graft, removal of cardiac tumors and so on. But performing surgery on a beating heart through “pinholes” is technically more difficult than working on a heart that has been stopped with the help of the heart-lung machine due to the lack of clear image guidance and the movement of heart. In addition, the stress on the heart during the procedure may lead to more heart muscle damage, lower blood pressure, irregular heart beat and potentially, brain injury if blood flow to the brain is reduced for too long during surgery. In average, 20% - 30% cases are converted to conventional heart surgery methods on an emergency basis.

In this project, we aim to develop model-based registration of 3D deformable objects (preoperation) to one or more 2D views (during the operation) of the scene to guide the robotical assisted heart surgery. Successful non-rigid 2D-3D registration requires a prior knowledge about biomechanical type of deformation as well as a prior knowledge about statistical type of deformation, and therefore we propose the development of integrated statistical and biomechanical motion models that will enable us to learn and predict the types of deformations that are most likely to occur. The integration of biomechanical models will be crucial if we are to account for changes in motion patterns as a result of deformations during surgery (e.g. changes in respiratory motion patterns as a result of the deflation of the left lung). My work is to build the patient-specific left ventricle and coronary arteries motion model from pre-operative images, and then to extend the developed techniques to construct generic models from a group of patients and healthy volunteer scans.

2 4D Left Ventricle Modeling

One problem area in minimally invasive cardiac surgery is the lack of 3D visualization for planning and guidance. This can be addressed by providing the surgeon with subject-specific geometric models (derived from 3D pre-operative images) that can then be used to plan port locations, to determine the best approach, or to rehearse a particular difficult case. For guidance purposes, these models can also be registered to the subject using 2D intra-operative images.

The purpose of this project is to develop an image-guided minimally invasive cardiac surgery system using a surgical robot. The key research issue which we will pursue in this project is the development of novel model-based 2D-3D registration techniques for matching 3D deformable objects such as the

heart as well as vessels to 2D endoscopic video images. This registration will enable us to establish the relationship between the 2D endoscopic video images seen by the surgeon and the patient's anatomy. We propose to superimpose models derived from preoperative image data onto the live 2D endoscopic video images. This will allow the surgeon to utilise preoperative tomographic data to accurate localise and track targets during the operation.

My work focus on building accurate left ventricle motion tracking model with pre-operative images, such as untagged MR, tagged MR and CT images. First, a static LV model is constructed via subdivision methods. Second, nonrigid multiframe lattice free form registration is used to build the motion tracking model. A static LV model built on tagged MR images is shown in Figure 3. The current models built on the above three image modalities can reasonably accurately mimic the motion of left ventricle.

2.1 Methods

Subdivision lattices are based on the idea of the recursive refinement of an initial base lattice according to a set of topological and geometrical rules. When these rules are applied, a sequence of lattices will be generated. The subdivision lattice will converge to a volume of space. The subdivision based methodology enables deformations to be described using a minimal set of parameters which we have utilized to model the deformation of the heart and develop an image registration algorithm for cardiac motion tracking.

Two sets of registrations are used to do the motion tracking, a set of point-surface registrations to create and initially align the model of the left ventricle which is then followed by a set of volumetric registrations to do the motion tracking.

The point-surface registration is achieved using a semi-automated procedure. First, a user places point markers on endocardium and epicardium of the left ventricle at one time point (end-diastole) in a set of short-axis and long-axis four-dimensional volumetric image sequences. Then, a set of template subdivision surface models of the endocardium and epicardium are registered to the point markers by minimizing the distances from the point markers to the surfaces. Endocardial and epicardial subdivision surfaces define the inner and outer boundaries of the subdivision lattice model of the left ventricle.

A sequence of volumetric registrations are then done to reconstruct the motion field from the pre-operative images. The motion of a point in the myocardium over time is calculated by registering the images taken during systole to the set of reference images taken at end-diastole. Registration is achieved by optimizing the positions of the vertexes in the base lattice so that the mutual information of the images being registered is maximized.

Figure 3 shows the left ventricle subdivision procedures. From top to bottom, left to right, the images are ordered sequentially (1-6).

Image 1 shows a template subdivision surface containing 25 vertices in the polygon mesh, which will be registered to the endocardial markers. In image 2, the approximate positions of the apex, base and septum are specified to calculate a homogeneous transformation matrix. This matrix is used to align the template surface with the endocardial markers initially. The displacements of the control vertices in the base polygon mesh are found by point-surface registration which minimizes the distances between

the point markers and the surface. As shown in image 3, the endocardial surface is constructed. The endocardial surface is then duplicated and registered to a set of markers delineating the epicardium, as in images 4 and 5. The corresponding vertices in endocardial and epicardial surfaces are then connected together to create the left ventricle subdibision lattice (image 6).

2.2 Research issues

Compared with MR images, CT images have much lower contrast, as shown in Figure 4. This cause the above standard methods not suitable for tracking cardiac motion in CT images. The volume of left ventricle changes dramatically which doesnot follow the real motion closely. See Figure 5. The first column is long axis view, second column is short axis view. This problem is caused by procedures in stage 2 when the static model is registered to all following frames in CT dataset. This happened because of the fundamental techniques of CT imaging. To address this problem, we propose three approaches. One is to add constraints to the motion tracking approaches. Second is to combine the cardiac segmentation and registration together. Third, the deformation information is collected from non-rigid free from registration in the original CT datasets and then is used to transform the static left ventricle lattice model from first frame.

2.2.1 Penalty

Penalties can be added to the registration process to preserve the volume to ensure the image transforms smoothly.

As the human body is made up of over 70% water, most tissues in the human body can be considered as incompressible. Therefore, a volume conservation penalty is beneficial to constrain the space of allowable transformations. Three approaches are done for this problem. One is to to preserve the volume of individual cell in each frame. In order to do this, we need to compute the volume of all cells and choose the suitable weighting for this penalty. We use two types of geometrical cells, hexahedron and tetrahedron. The volume of any tetrahedron, given its vertices a, b, c and d is

$$V = \frac{|(d-a)\cdot((d-b)\times(d-c))|}{6}.$$

Since a hexahedron can be divided into five tetrahedra, we can also use this equation to caculate the volume of hexahedron.

We formulate the penalty term as

$$penalty = weight * \frac{1}{N}\sum_{i=1}^{N}\frac{(v_{i_{initial}} - v_i)^2}{(v_{i_{initial}})^2}$$

where $v_{i_{initial}}$ is the volume of the i_{th} cell in the original subdivision lattice and v_i is the correponding volume in the current lattice. N is the number of cells.

Second approach is to preserve the whole volume of the subdivision lattice in each frame. The formulation is:

$$penalty \;=\; weight \;*\; \frac{\left(V_{initial} - \sum\limits_{i \in cells} v_i\right)^2}{\left(V_{initial}\right)^2}$$

where $V_{initial}$ is the volume of the original subdivision lattice, v_i is the volume of cell i in the current transformed lattice, $weight$ is the user defined penalty weighting.

Thirdly, we measure the local relative volume change of the transformation field by using the determinant of the Jacobian matrix at the point x,

$$J_T(\mathrm{x}) = det \begin{pmatrix} \frac{\partial T_x(x)}{\partial x} & \frac{\partial T_x(x)}{\partial y} & \frac{\partial T_x(x)}{\partial z} \\ \frac{\partial T_y(x)}{\partial x} & \frac{\partial T_y(x)}{\partial y} & \frac{\partial T_y(x)}{\partial z} \\ \frac{\partial T_z(x)}{\partial x} & \frac{\partial T_z(x)}{\partial y} & \frac{\partial T_z(x)}{\partial z} \end{pmatrix}.$$

$$If\ J_T(\mathrm{x}) \begin{cases} < 1 & compression\, in\, a\, small\, neighborhood\, of\, \mathrm{x} \\ = 1 & incompressible \\ > 1 & expansion\, in\, a\, small\, neighborhood\, of\, \mathrm{x} \end{cases}$$

This incompressibility penalty term $\mathcal{C}_{Jacobian}$ penalizes local tissue expansion and compression,

$$\mathcal{C}_{Jacobian} = \frac{1}{N_P} \sum_{\mathrm{x} \in P} |\, log\left(J_T(\mathrm{x})\right) |\ ,$$

where P is the set of control points. This penalty is nonnegative, and has its minimum value of zero when the value of the Jacobian is unity.

2.2.2 Segmentation

Using expectation maximum algorithm, the coronary CT images are classified into different types. In three types approach, myocardium, blood pool, background are differentiated. In four types approach, the outer linning of the myocardium is added. See Figure 6 for the myocardium segmentation in 8 time frames.

Figure 6: Myocardium

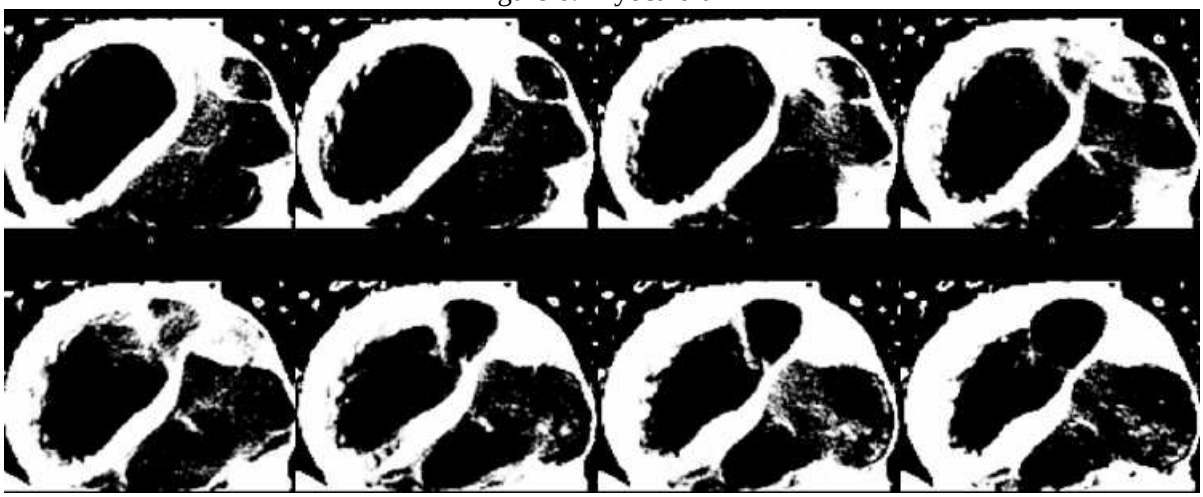

2.2.3 Lattice transformation

In this approach, non-rigid image registration is done across the time frames in the CT datasets. Four different similarity measures, namely, cross correlation, mutial information, normalized mutual information and sum of squared distance, are used. We then use the collected transformation information to deform the lattice rather than using lattice free form registration method. Figure 7 shows the motion model constructed with cross correlation captured in 20 frames.

Figure 8shows the volume change of model in each similarity measure.

3 4D Coronary Artery Modelling

4D models of coronary artery tree is a valuable help for the planning and simulation of minimally-invasive cardiac surgery. For example, the robotically assisted totally endoscopic coronary artery bypass avoids the opening of the thorax and limits post-operative consequences. On the other hand, the confined vision delivered by the endoscope greatly increases the difficulty of locating the coronary arteries. If we could construct a 4D model of the coronary artery tree from pre-operative images, then we could use the model to enhance the surgeon's endoscopic vision and help him to find the planned operative position on the correct artery in the surgical context.

The plan for this part of project is to construct patient-specific coronary artery motion model from preoperative CT scans. Right coronary artery, left coronary artery, left anterior descending coronary artery, circumflex coronary artery and left internal mammary artery (Figure 9) are all extracted and constructed from CT image datasets. Then the coronary anatomy and motion model both are obtained from coronary CT images.

About the vessel extraction, two different approaches are used. First, manual extraction is done in each dataset, which is very laborious, but accurate and can be used as reference. Second one is semi-automatic. We apply a ridge detection based vessel extraction algorithm to detect centerlines throughout cardiac vasculatures. Seed generation algorithm is used to automate the extraction process and to achieve

the extraction of complete coronary arteries. Efficiency of the method is improved by only employing seeds near vessels. Seeds can also be placed manually if a specific artery is to be segmented.

Figure 10 illustrates the coronary arteries extracted from one frame.

Finally, after fusion with the left ventricle motion model obtained in Section 2, the coronary artery tree motion model will be integrated in a planning and simulation system for robotically assisted surgery and its real-time registration with endoscopic images in the operating context will guide the surgeon's gesture by augmented reality. Future improvement will make applications to diagnostic and follow-up of the cardiac diseases possible.

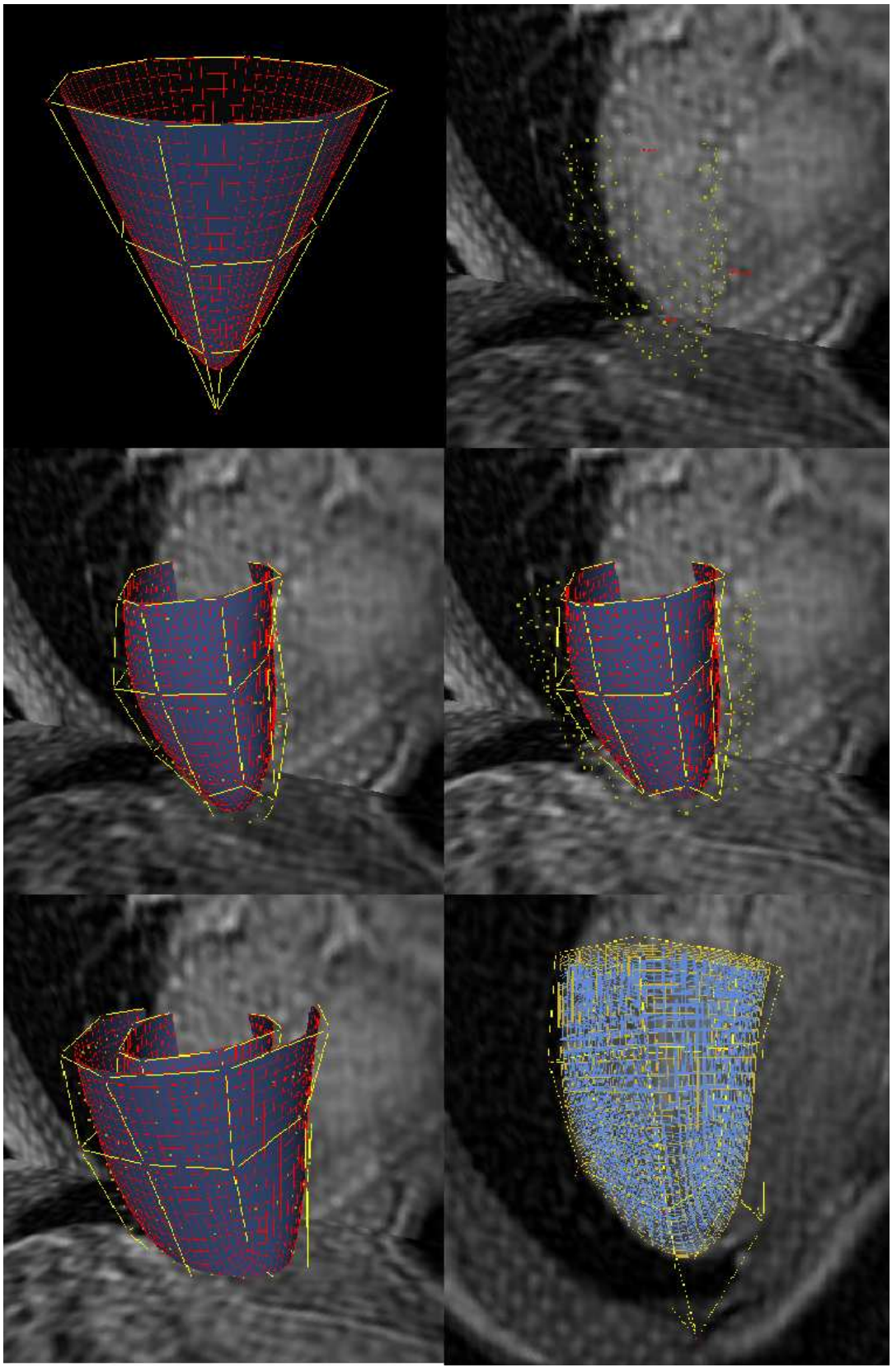

Figure 3: Left ventricle subdivision model from tagged MRI

Figure 4: MRI & CT

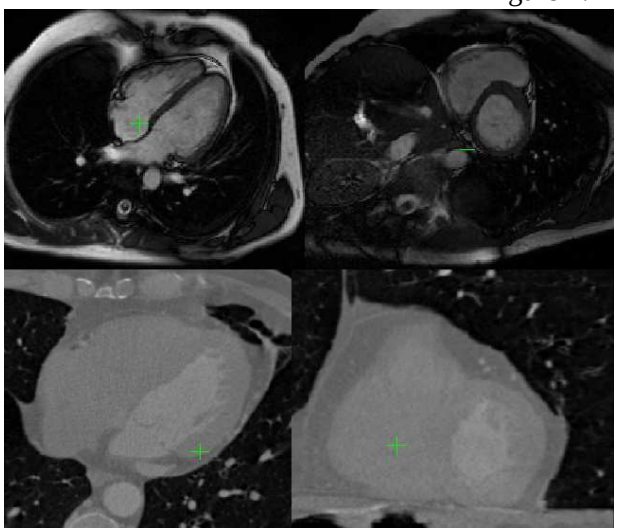

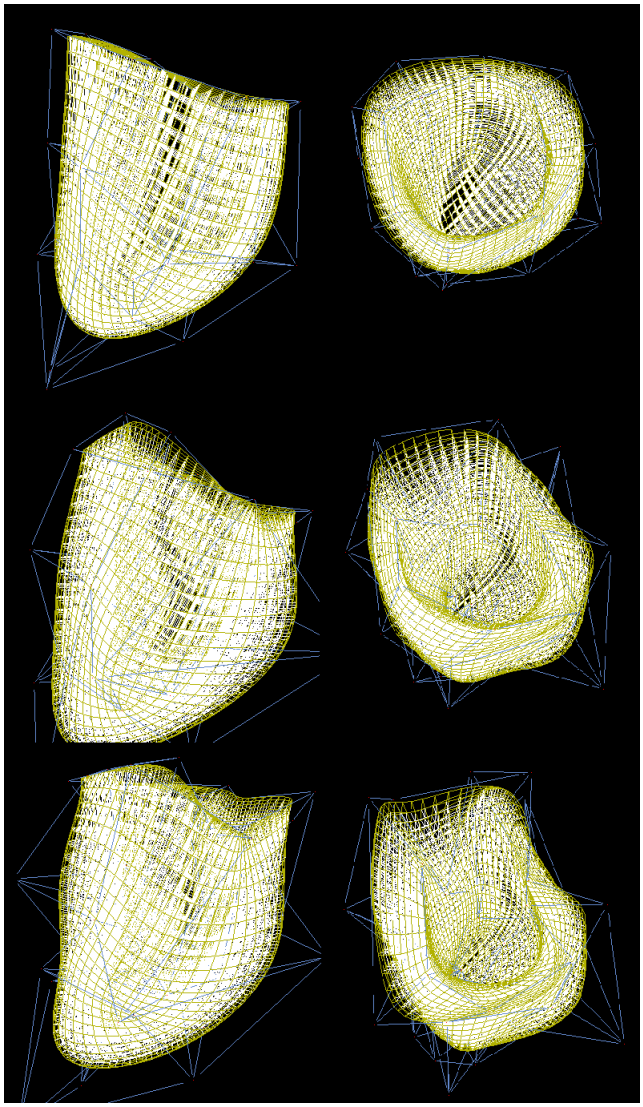

Figure 5: Left ventricle motion model from CT images

Figure 7: Motion Model from CT images

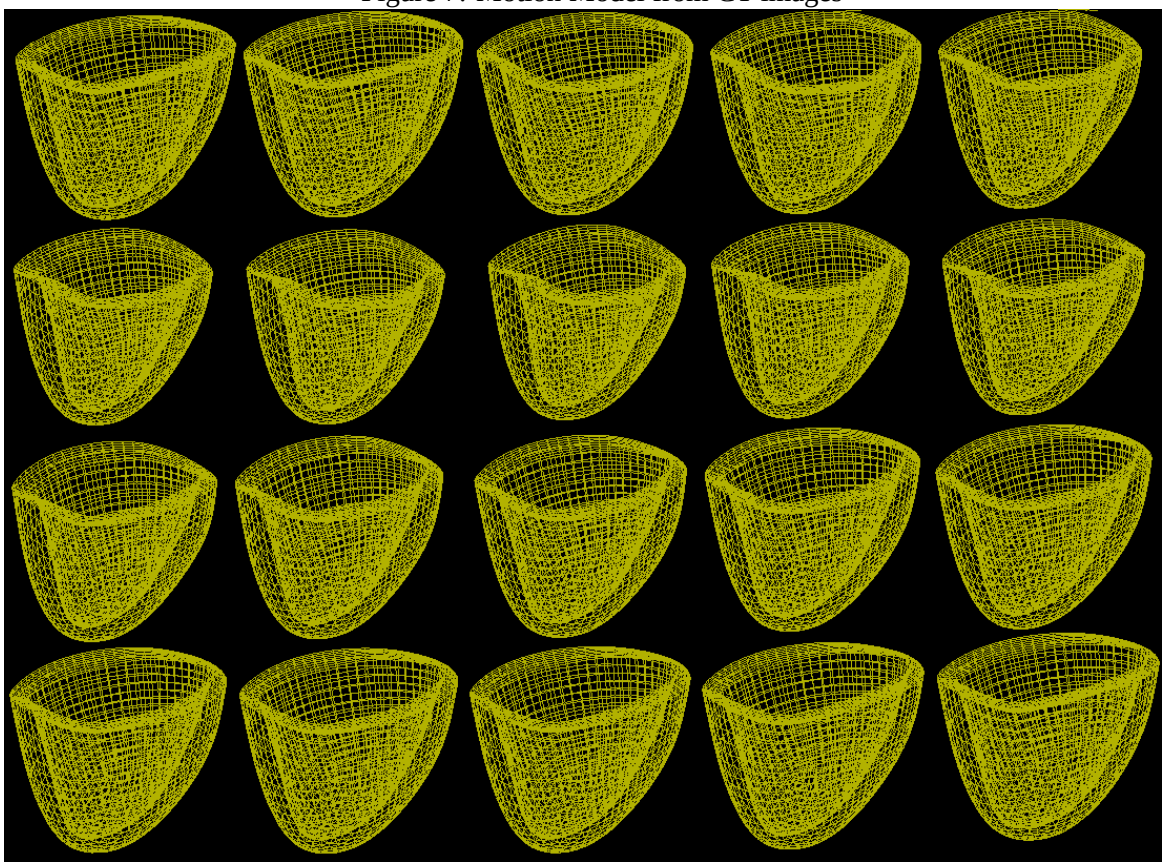

Figure 8: Volume Changes

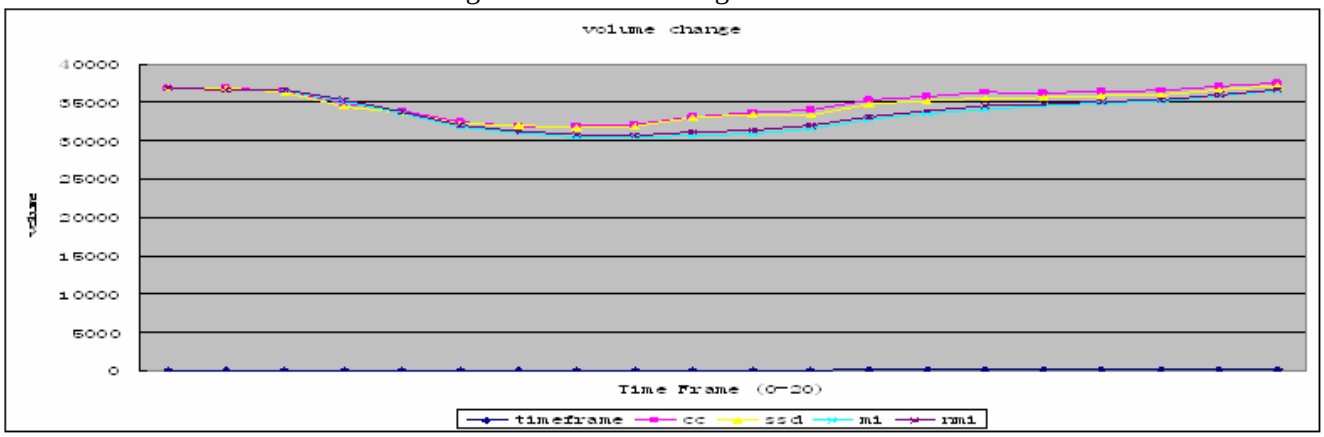

Figure 9: Coronary arteries

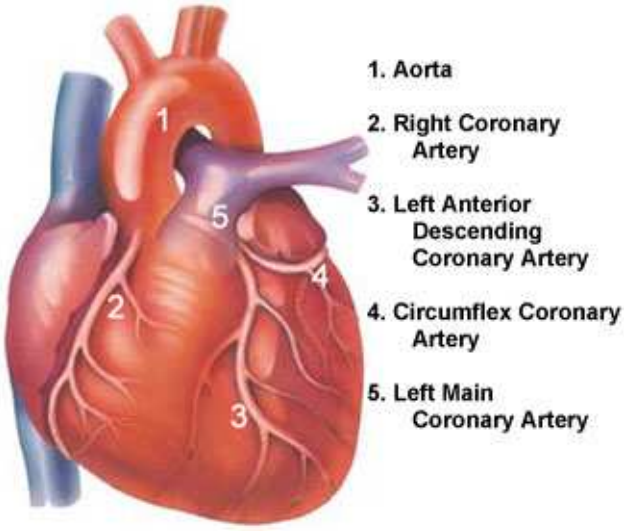

Figure 10: Coronary Arteries and LIMA